ISSN 2630-0958

Journal de Physique de la Soaphys

J. P. Soaphys

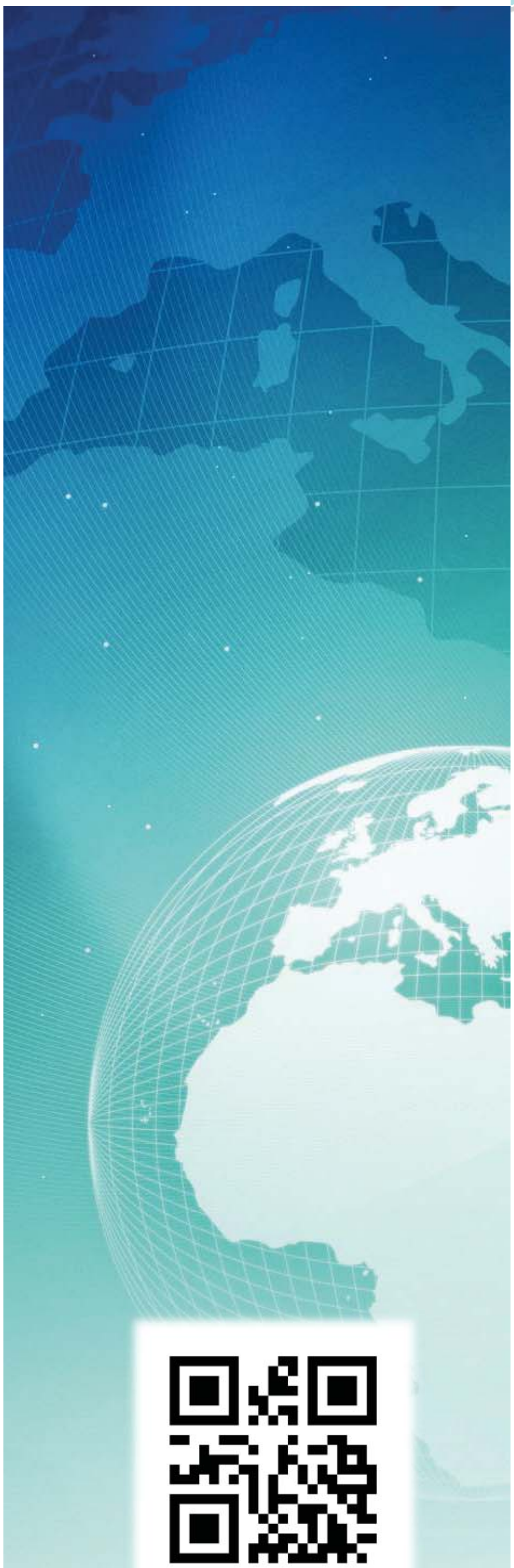

Volume 2, Numéro 2 - Décembre 2020

Journal de Physique de la Soaphys
Volume 2, Numéro 2, Décembre 2020

Journal de Physique de la Soaphys
Volume 2, Numéro 2, Décembre 2020

SOMMAIRE

J. P. Soaphys, Vol 2, N°2 (2020) C20A22
http://dx.doi.org/10.46411/jpsoaphys.2020.02.22

Journal de physique de la SOAPHYS
http://www.soaphys.org/journal/
ISSN Print : 2630-0958

ADAPTIVE PROPORTIONAL INTEGRAL CONTROLLER BASED ON ANN FOR DC LINK VOLTAGE CONTROL SINGLE-PHASE INVERTER CONNECTED TO GRID

Traore Mamadou[1], Ndiaye Alphousseyni [1], Ba Amadou [1], and Mbodji Senghane [2]

[1]*Research Team Energetic System and Efficiency, Alioune Diop University of Bambey, Bambey, Senegal,* mamadoutraore1uadb@gmail.com, mamadou.traore@uadb.edu.sn, alphousseyni.ndiaye@uadb.edu.sn,

[2]*Research Team Renewable Energies Materials and Laser, Alioune Diop University of Bambey, Bambey, Senegal,* senghane.mbodji@uadb.edu.sn,

INFOS SUR L'A R T I C L E

Historique de l'article:
Reçu le : 26 novembre 2020
Reçu en format revisé le : 18 février 2021
Accepté le : 23 avril 2021

Keywords : *PI-ANN Contoller, PV, Inveter, Grid.*

A B S T R A C T

The output power of the inverter of a PV system is directly affected by the DC-link voltage. Hence an adaptive Proportional Integral controller based on Artificial Neural Networks is developed in this paper. MATLAB/Simulink is used for the simulation of the studied system in order to evaluate the performance of the proposed methods. Simulation results show that the proposed API-ANN is faster to track the DC-link voltage than the conventional method. The injected harmonics to the grid were significantly reduced with API-ANN (0.08 % of total harmonic distortion) in comparison with the classic PI with 4.23 %. The API-ANN gives a good performance than the classic PI.

I. INTRODUCTION

During the last decade, the dependance of the energy sector is dominantly depended on renewable energy sources [Kumar et al., 2019]. The latter is playing a capital role in the energy production to reduce green gas emission (air pollution), energy supply and security and environmental protection [Cao et al. 2020; Baba et al., 2020]. The photovoltaic (PV) solar panels is one of the most important clean sources [Mostafa et al., 2020, Baba et al., 2020]. According to the global photovoltaic solar panels market outlook, 2019-2023, the capacity of installed solar power generators in the world may reaches 1610 GW in 2023 [Mao et al., 2020]. In order to achieve the climate goals of 2015 Paris Agreement defined [Roth et al., 2020], the government of Senegal promotes the mix energy particularly the photovoltaic system. From 2016 to 2020, 102 MW of PV power have been installed [Ndiaye et al., 2020]. The photovoltaic systems connected to the grid is an ideal solution for peak energy demand [Meddour et al., 2019]. The high penetration of distributed energy has increased the demand for single-phase inverter grid [Arun et al, 2013; Azab, 2020] and it is the most commonly used. The non-linear characteristic of the output of the PV system makes it necessary to obtain the MPPT operation [Mostafa et al., 2020].

The DC Link voltage (interface PV system and inverter) directly affects the output power of the inverter. In the literature, various techniques of control are used. There are the classic and the intelligent methods. Hence a hysteresis Neutral Point-Clamped (NPC) control and proportional based NPC control are proposed for suppression of DC-link voltage unbalance [Porru et al, 2018]. Simulation results showed that in terms of minimum switching losses, hysteresis is better than P-based NPC and in terms of minimum DC-link voltage the P-based NPC is recommended. In Ba *et al*, research work [Ba et al, 2020], the proportional integral (PI) and the proportional integral derivative (PID) are used to maintain constant the DC bus voltage of a PV-Battery system connected to the grid. It is shown that the PID controller is more performant than the PI controller.

Further, a novel Space Vector Modulation (SVM) is used to reduce the total harmonic distortion (THD) by Najafi et al [Najafi et al, 2019]. Simulation results validated that the SVM allowed to obtain 1.76 % of THD. An adaptive neural networks is used to optimize and turn the controller parameters [Mohamed et al, 2019]. This technique allowed to reduce the THD of 1.97 %. A high DC-link voltage bandwidth (DCL-BW) is also proposed [Zarei et al, 2020]. This method is based on output current harmonic distortion. The simulations' results showed that the DCL-BW enhances the power quality indices of the grid-connected inverter with THD below 3.5 %.

To regulate the DC bus voltage of a stand-alone DC microgrid, a novel distributed control based on direct Lyapunov method is done [Abedi et al, 2020]. The performance of the proposed technique achieved the desired DC bus, accurate current generation and supplying load appropriately with fast dynamic responses. Furthermore, an Artificial Neural Network of Dynamic Voltage Restorer (ANN-DVR) is developed to improve the performance of a stand-alone hybrid renewable energy [Prabaharan et al, 2019]. It is remarked that the ANN-DVR method improve the voltage of 0.86%, the current and the power waveforms. Moreover, a command approach is proposed to rise the DC-link voltage and the output current of the inverter, respectively [Hamrouni et al, 2019]. It is noted that the DC-link voltage is maintained constant and the current with a low THD is injected into the grid. All the works discussed above are studied on controlling the DC-link voltage or the output current of the inverter connected to the grid. These authors have used some classic and intelligent methods but they did not use intelligent techniques to control the DC-link voltage in order to improve energy quality. Therefore, in this paper, an Adaptive Proportional Integral controller based on Artificial Neurol Networks (API-ANN) and classic PI are proposed to control the DC Link voltage and the power injected into the grid under MATLAB/Simulink of a system composed by PV panels and single-phase inverter connected to the grid. The PI calculates the probability of drop using the error and integral of the error between the current queue size and the desired queue length. ANNs are computational models inspired by the human brain and they work just like a functioning human nervous system. In recent years, the ANNs have become useful and competent modelling tools, especially for modelling the environmental processes that are difficult to identify physically or statistically methodologies and controls [Seketekin et al., 2020; Hussain et al., 2020; Wanga et al., 2020].

The main purpose of this work is to maintain the DC Link voltage in order to inject a good quality of energy to the grid and to obtain a low Total Harmonic Distortion (THD). To measure the performance of API-ANN and classic PI, the mean absolute square percentage error (MAPE), the mean absolute error (MAE) and the root mean square error criterias are used. This document is organized as follows:

Section 2 and 3 describe the studied system and the API-ANN and PI controllers, respectively.

In section 4, simulation results and discussions are developed,

Finally, a conclusion will be made in section 3 of this paper.

II. PROPOSED SYSTEM

The proposed system is shown in figure 1. It is composed by PV panels, and a single-phase inverter connected to the grid.

The rest of the system is the system's control. The latter is applied to regulate the voltage of the DC Link panels and the output current of the inverter in order to inject a good quality of energy.

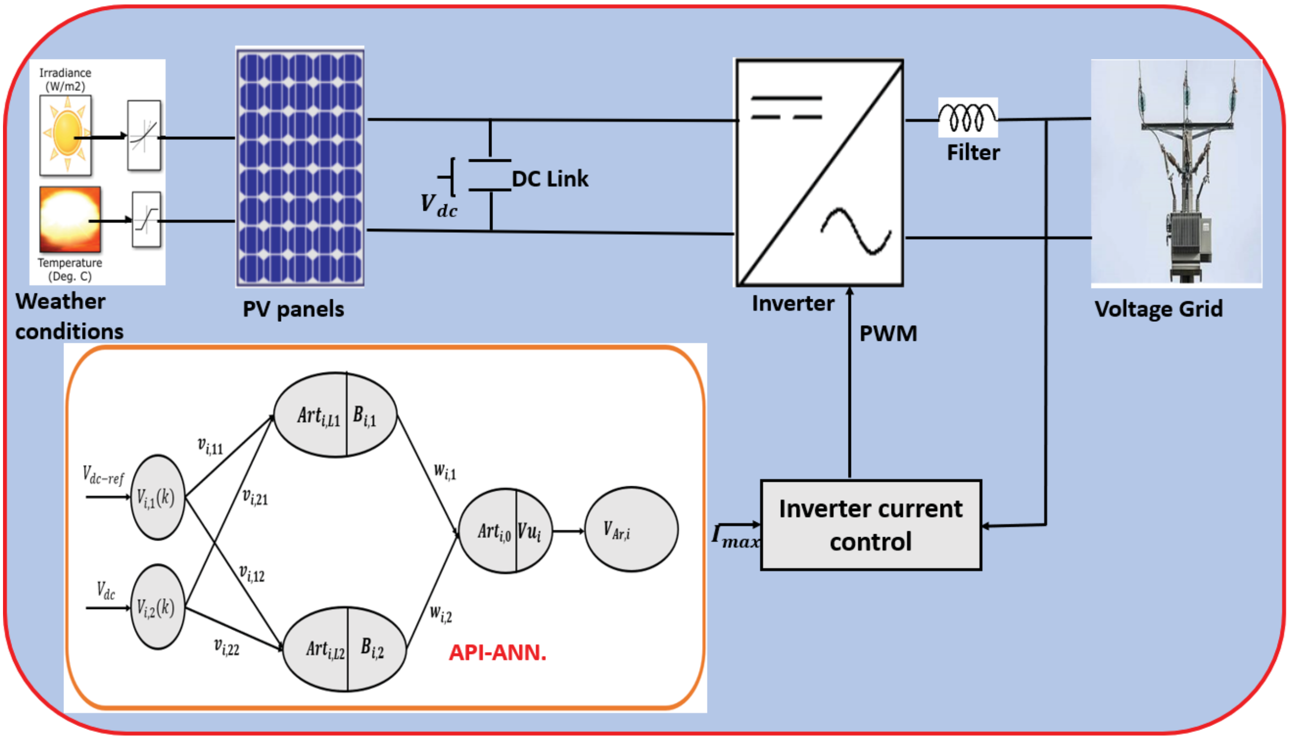

Fig.1: Schematic diagram of the studied system

III. CONTROL

The objective of the control is that the average value of DC Link voltage be equal to its reference value. Because, the output power of a voltage source inverter of a PV system is directly influenced by the DC-link voltage. Equation (1) gives the amplitude of the DC Link voltage. Where i_{dc} and C_{dc} represent respectively the DC-link current and the DC-link capacity.

$$V_{dc} = \frac{i_{dc}}{C_{dc} \cdot p} \quad (1)$$

The parameters of the PI controller are the proportional gain k_P and the integral gain k_I PI calculates the probability of drop using the error and integral of the error between the current queue size and the desired queue length. The transfer function of PI controller is given by equation (2):

$$F_{PI}(p) = k_P + \frac{k_I}{p} \quad (2)$$

The challenge of classic PI controller is to obtain the appropriate value of its parameters.

Therefore, we used the API based on Artificial Neural Networks (API-ANN). The figure 2 represents the PI Neural Networks proposed. Its structure consists of two inputs that are the DC-link reference voltage (V_{dc-ref}) and the DC-link detected value (V_{dc}) and one output which gives the optimal value of current provided by the control system.

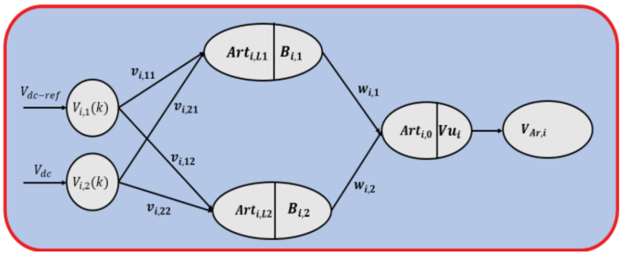

Fig. 2: PI Neural Networks

This figure 2 is composed of fours layers. It is described as follows:

-$V_{i,1}(k)$ and $V_{i,2}(k)$ are the normalized references and the detected voltage values, respectively;

-$Art_{i,L1}(k)$ and $Art_{i,L2}(k)$ are the input values of neurons in the first hidden layer;

-$B_{i,1}(k)$ *and* $B_{i,2}(k)$ are the status transfer function of proportional and integral neurons, respectively;

-$Art_{i,0}(k)$ and V_{ui} are the input and output values of the second hidden layer.

These physical quantities are defined below:

$$V_{i,1}(k) = g\left(\frac{V_{dc-ref}}{V_{dcmax}}\right) \quad (3)$$

$$V_{i,2}(k) = g\left(\frac{V_{dc}(k-1)}{V_{dcmax}}\right) \quad (4)$$

$$Art_{i,Lj}(k) = \sum_{L=1}^{2} v_{i,Lj} V_{i,Lj}(k) \text{ with j=1, 2.} \quad (5)$$

$$B_{i,1}(k) = g(Art_{i,L1}(k) - Art_{i,L1}(k-1)) \quad (6)$$

$$B_{i,2} = g(Art_{i,L2}(k)) \quad (7)$$

$$Art_{i,0}(k) = \sum_{j=1}^{2} w_{i,j} B_{i,j}(k) \quad (8)$$

$$V_{ui}(\mathrm{k}) = V_{ui}(\mathrm{k}-1) + g(Art_{i,0}(k)) \quad (9)$$

$$VAr_{,i}(\mathrm{k}) = V_{ui}(\mathrm{k}) Z_i(\mathrm{k}) \quad (10)$$

Z_i(k) in equation (10) is the error variance ratio. It is used to modify V_{ui} (k).

$$Z_i(k) = \begin{cases} 1 & abs\left(erri(k-1)\right) > F_x \\ \dfrac{erri(k-1)^2}{\sum_{i=1}^{n} erri(k-1)^2} & abs\left(erri(k-1)\right) \leq F_x \end{cases}$$

$$erri(k-1) = V_{dc-ref}(k-1) - V_{dc}(k-1)$$

F_x is the threshold of voltage deviation and n is the number of the wires.

The gradient-based back-propagation algorithm which is
modified by the error variance ratio to reduce the effect of disturbance and enhance the learning efficiency is the leaning method in this paper. The parameters between input layer and output layer are updated by:

$$v_{i,j}(k+1) = v_{i,j}(k) - \beta \frac{\partial E_i}{\partial v_{i,j}} \quad (11)$$

$$\text{With} \quad E_i = \left(\frac{V_{dc-ref}(k) - V_{dc}(k)}{V_{dcmax}}\right)^2 \quad (12)$$

β is the learning rate between input layer and the first hidden layer. is the learning rate between the output layer and the first hidden layer.

Table 1 gives the parameters of the PV panels and the classic PI

Table 1: Parameters of PV panels and Classic PI

Parameters	Value
Numbers of Panels	14
Open circuit voltage (V)	37.6
Voltage at maximum power point (V)	31
Short-circuit current (A)	8.55
Current at maximum power point (A)	8.06
Proportional gain k_P	0.912
Integral gain k_I	204.74

IV. RESULTS AND DISCUSSION

Figures 3 presents the voltage versus the times considering the DC Link control by PI-ANN, the DC Link control by PI Classic and DC Link control by PI-ANN and Classic PI.

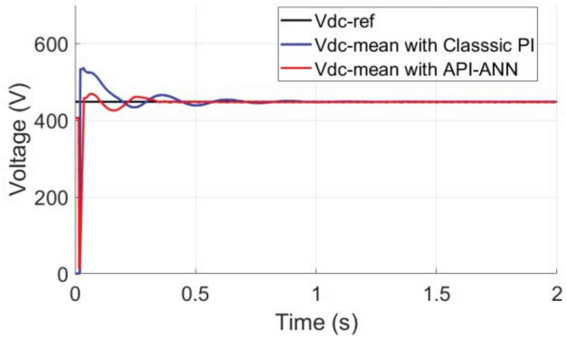

Fig. 3: DC Link control by PI-ANN and Classic PI.

The results on figures 3 is obtained after the simulation under Matlab /Simulink. The simulation time is fixed at two (2) seconds. This figure shows that the methods used make it possible to quickly reach the DC link reference voltage. There are oscillations of the DC link measured voltage. With PI-ANN the oscillations are minimal and the overshoot is not as great as with classic PI.

Figure 4 is a obtained from figure 3, which is used to determine the overshoot and response time. These are shown in the table 2.

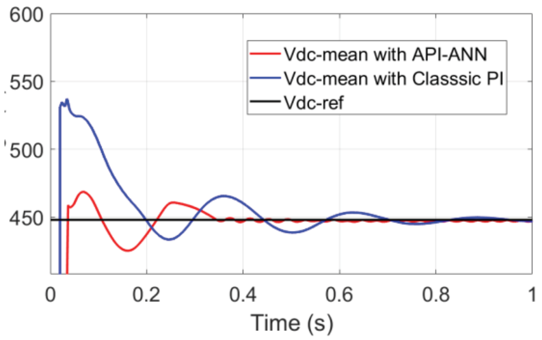

Fig. 4: DC Link control by PI-ANN and Classic PI.

Table 2: Some Criteria of regulation

Criteria	Classic PI	API-ANN
Overshoot (%)	21.77	2.22
Response time (s)	0.01	0.015

Table 3: API-ANN controller parameters

DC-link Voltage (V)	k_P	k_I
425	5.661	45.06
430	8.66	46.43
437	11.15	47.91

The table 3 gives the API-ANN parameters for different values of DC-link voltage.

Figures 5 and 7 show the injected current and the reference current with the proposed methods.

The figures 6 and 8 give the total harmonic distortion (THD) obtained with API-ANN and Classic PI controllers.

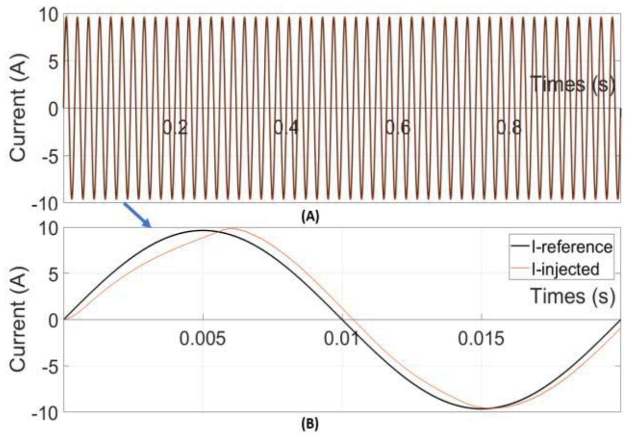

Fig.5: Injected current and its reference regulated by Classic PI.

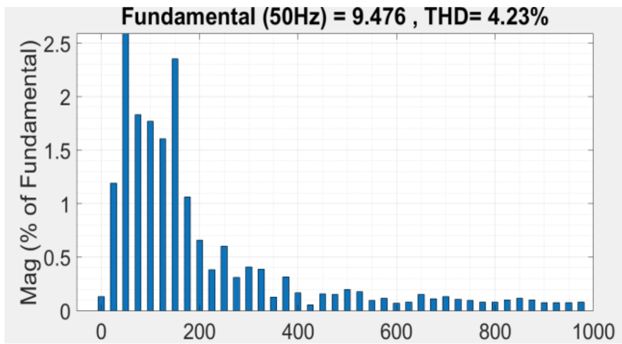

Fig. 6: Total Harmonic Distortion with Classic PI.

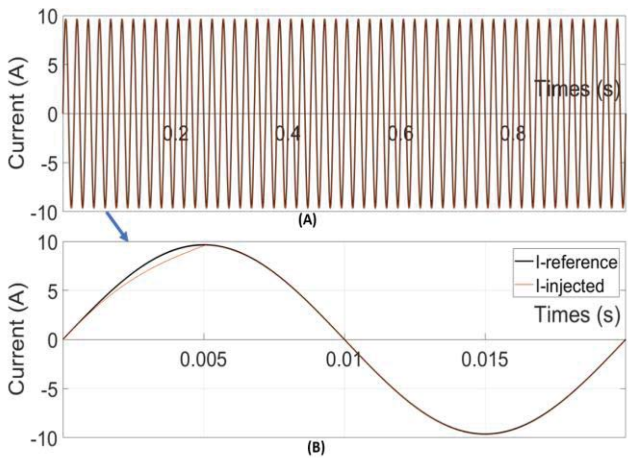

Fig. 7: Injected current and its reference regulated by API-ANN.

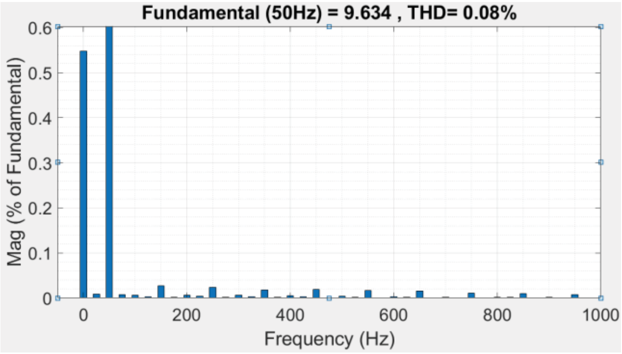

Fig. 8: Total Harmonic Distortion with API-ANN

It is remarked in figures 5 (B) and 7 (B) that, excepted 0.0025 second of the simulation's times, the injected current follows correctly the reference current with API-ANN.

Figures 6 and 8 show that the system injected a good quality of power with API-ANN. Because we obtain 0.08 % and 4.23 % for API-ANN and classic PI, respectively.

To measure the performance of API-ANN and Classic PI, some criteria are used:

The RMSE, MSPE and MAE are also used to make a difference between API-ANN and classic PI and to know which methods is more performant.

The mean absolute square percentage error (MAPE) gives an idea of how the measurement of the relative sizing of one physical quantity is well measured. In this work the latter is the injected current (I_{in}). Its expression is given by equation 12:

$$MAPE = \frac{1}{N}\sum_{k=1}^{N}\left|100(\frac{I_{in}(k)-I_{ref}(k)}{I_{in}(k)})\right| \quad (12)$$

The mean absolute error (MAE) gives accuracy percentage and a low percentage of this parameters indicates a good model performance. Equation 13 gives its expression:

$$MAE = \frac{1}{N}\sum_{k=1}^{N}\left|(\frac{I_{in}(k)-I_{ref}(k)}{I_{in}(k)})\right| \quad (13)$$

The root mean square error gives the lowest value. It is calculated by equation 14:

$$RMSE = \sqrt{\frac{1}{N}\sum_{k=1}^{N}(I_{in}(k) - I_{ref}(k))^2} \quad (14)$$

The physical quantity measured now is the output current of the single-phase inverter. Table 4 gives the results of the calculation.

Table 4: Performance of classic PI and API-ANN

Methods	RMSE	MAPE	MAE
Classic PI	0.7307	1.8979	0.0190
API-ANN	0.0572	0.7272	0.0073

The values in table 2 show that the API-ANN is more performance than the classic PI. Hence, the use of the proposed technique is very important and improves greatly the performance of the system.

In recapitulation, the API-ANN is better than the classic PI to control the DC Link voltage.

V. CONCLUSION

In this paper the control of the DC Link voltage and the output current of a single-phase inverter connected to the grid have been developed. Classic PI and API- ANN are proposed to regulate the DC Link voltage. The novelty of our work consisted in the improvement of the quality of the energy by reducing in a consequent way the THD using API-ANN controller.

For this purpose, simulation results show that the API-ANN is best to control the DC Link voltage. Hence, the proposed technique allowed to obtain 0.08 % of THD. So, the system is compatible with the requirements in the IEEE 519 international standard for harmonic control in electrical power systems (THD ≤ 5 %).

ACKNOWLEDGEMENT

The authors thank the Renewable Energies Materials and Laser and the Efficiency and Energy System research teams of Alioune Diop University of Bambey (Senegal).

REFERENCES

Abedi, A., Rezaie, B., and al., 2020. *DC-bus Voltage Control based on Direct Lyapunov Method for a Converter based Stand-alone DC Micro-grid".* Electric Power Systems Reseach, Vol. 187, 106451.

Arun, K., and Selvajyothi, K., 2013. *Observer Based Current Controlled Single-Phase Grid Connected Inverter*". Procedia Engineering, Vol. 64, 367 – 37.

Azab, M., 2020. *Multi-objective design approach of passive filters for single-phase distributed energy grid integration systems using particle swarm optimization*". Energy Reports, Vol. 6, 157–172.

Ba, A., Ndiaye, A., Mbodji, S., 2020. *Supervision Strategy of a Hybrid System PV with Storage for Injection to the Electrical Network".* https://doi.org/10.1007/978-3-030-51051-0_10, Vol. 321, 134-145.

Baba, A. O. Liu, G. Chen, X., 2020. *Classification and Evaluation Review of Maximum Power Point Tracking Method",* Sustainable Futues, Vol. 2, 100020.

Cao, Y. Yao, H. Wang, Z., 2020. *Optimal Designing and Synthesis of a Hybrid PV/Fuel cell/Wind System using Meta-heuristics",* Energy ReportsVol. 6, 1353-1362.

Hamrouni, N., Younsi, S., Jraidi, M., 2019. *A Flexible Active and Reactive Power Control Strategy of a LV Grid Connected PV System".* Energy Procedia, Vol. 162, 325–338.

Hussain, M., Dhimish, M., and al., 2020. *Artificial Neural Networks based Photovoltaic fault detection algorithm integrating two bi-directional parameters"*. Renewable Energy, Vol. 155, 1272-1292.

Kumar, V. Sing, M., 2019. *Sensorless DC-link control approach for three-phase grid integrated PV system",* Electrical Power and Energy system, Vol. 112, 309-318.

Mao, M. Cui, L., 2020. *Classification and summarization of solar photovoltaic MPPT techniques: A review based on traditional and intelligent control strategy*". Energy Report, Vol. 6, 1312-1327.

Mohamed, A. A. S., Metwally, H., and al., 2019. *Predictive neural network based adaptive controller for grid-connected PV systems supplying pulse-load"*. Solar Energy, Vol. 193, 139-147.

Mostafa, M. R Saad, N. H., 2020. *Tracking the maximum power point of PV array sliding mode control method".* Ain sham engineering Journal, Vol. 11, 119-131.

Najafi, P., Viki, H. A., and al., 2019. *Novel space vector-based control scheme with dc-link voltage balancing capability for 10 switch converters in bipolar hybrid microgrid".* Sustainable Energy, Grids and Networks, Vol. 20, 100-256.

Ndiaye, E. M. Ndiaye, A. Faye, M., 2020. *Experimental Validation of PSO and Neuro-Fuzzy Soft-Computing Methods for Power Optimization of PV installation*". IEEE International Conference on Smart Grid, June 17-19, 2020, Paris, France.

Porru, M., Serpi, A., and al., 2018. *Suppression of DC-link voltage unbalance in three-level neutral-point clamped converters"*. Journal of the Franklin Institute, Vol. 355, 728–752.

Prabaharan, N., Campana, P. E., and al., 2019. *A new approach for grid integration of solar photovoltaic system with maximum power point tracking using multi-output converter".* Energy Procedia, Vol. 159, 521-526.

Rotha, S., Stumpe, L., 2020. *An optimization-based approach for the planning of energy flexible production processes with integrated energy storage scheduling*". Procedia CIRP, Vol. 88, 258-264.

Seketekin, A., Aslan, N., and al., 2020. *Modelling Diurnal Land Surface Temperature on a Local Scale of an Arid Environment Using Artificial Neural Network (ANN) and Time Series of Landsat-8 Derived Spectral Index".* Journal of Atmospheric and Solar–Terrestrial Physics, Vol. 206, 10532.

Wanga, F., Xuana, Z., and al., 2020. *A day-ahead PV power forecasting method based on LSTM-RNN model and time correlation modification under partial daily pattern prediction framework".* Energy Conversion and Management, Vol. 212, 112-766.

Zarei, F. S., Mokhtari, H., and al., 2020. *DC-link loop bandwidth selection strategy for grid-connected inverters considering power quality requirements".* Electrical Power and Energy Systems, Vol. 119, 105879.

Journal de Physique de la Soaphys
Volume imprimé avec la contribution de :